Hindawi
Advances in Civil Engineering
Volume 2023, Article ID 7974380, 16 pages
https://doi.org/10.1155/2023/7974380

Research Article

Study on Mechanical Effect and Plastic Zone Distribution of Tunnel Surrounding Rock in the Presence of Various Expansion Approaches

Bowen Duan [1] **and Jun Yang** [2]

[1]*School of Civil Engineering and Architecture, China Three Gorges University, Yichang, Hubei Province, China*
[2]*School of Civil Engineering, China Three Gorges University, Yichang, Hubei Province, China*

Correspondence should be addressed to Jun Yang; wangjing750301@163.com

Received 19 September 2023; Revised 28 November 2023; Accepted 30 November 2023; Published 26 December 2023

Academic Editor: Tariq Umar

To examine the distribution of the plastic zone of the surrounding rock subjected to various expansion approaches used for the existing tunnels, this article deals with the distribution and thickness of the plastic zone of the surrounding rock subjected to one-sided expansion excavation (1SEE), two-sided expansion excavation (2SEE), and surrounding expansion excavation (SEE). First, the mechanical model of tunnel expansion is established and the initial stress field 1SEE and expansion stress field of tunnel surrounding rock are analyzed. The finite element model of tunnel expansion is developed to examine the plastic zone distribution in the presence of various tunneling approaches. The obtained results reveal that with the growth of expansion size, the plastic distribution area grows, with a maximum increase rate of 138.5%; the difference of each position reduces, with the difference value of each part less than 0.2 m. The plastic zones of 2SEE and SEE approaches are almost symmetrically distributed around the tunnel center line, and the invert and vault of the SEE tunnel are excavated at the same time, the excavation size is the same, and the difference in plastic zone range is small. With the rise of the lateral pressure coefficient, the distribution pattern of the plastic zone changes from X-type to butterfly-type and then to ellipse-type.

1. Introduction

With the continuous development of the Chinese economy, and increasing traffic and transportation volume, many tunnels cannot meet the traffic requirements; therefore, tunnel expansion has become an effective way to solve the traffic bottleneck [1]. Tunnel expansion refers to the existing foundation, breaking the existing surrounding rock structure, expanding the tunnel section, and forming a new tunnel to meet the usage requirements [2]. Construction methods, processes, and support measures for tunnel widening significantly differ from those used in constructing new tunnels: they necessitate the destruction of existing tunnel support structures. Traffic requirements impose higher demands on construction timelines. This may require construction within the confines of preexisting land use planning, considering the effects on existing traffic, transportation systems, buildings, and subterranean facilities such as pipelines. Moreover, the internal force and the deformation characteristics of the surrounding rock are different from the new tunnel, and there is no specific design and construction specification for tunnel expansion in China. Facing the problem of tunnel expansion, we basically refer to the specifications of new tunnels. According to the existing tunnels in the early construction, the tunnel surrounding the rock has completed most of the stress release. In the construction process of the tunnel expansion refers to the support of the new tunnel, the overly conservative design will inevitably lead to a waste of costs. Further, various tunnel expansion approaches lead to various forms of stress release in the surrounding rock, forming different thicknesses and shapes of plastic zone, resulting in material strength reduction and deformation concentration in plastic zone. As a result, due to insufficient support, potential safety hazards may arise. Therefore, it is of great significance to examine the elastic–plastic zoning of existing tunnels in the presence of various expansion methods.

Researchers at home and abroad have conducted a lot of research in this field. Using the Mohr–Coulomb strength criterion, Zhang et al. [3] deduced the boundary equations of the plastic zone of rock around a circular tunnel under the condition of unequal pressure in both directions and analyzed the distribution shape of the plastic zone under different levels of the surrounding rock and the influence of the excavation radius on the plastic zone distribution. Wang et al. [4] utilized a theoretical analysis to examine the influence of the support structure on the plastic zone of the surrounding rock in circular tunnels, suggesting a suitable calculation approach accounting for the actual construction process, which can well consider the interaction between the surrounding and supporting structure. By choosing the Wuyi Tunnel of the Beijing–Fuzhou Railway as the research target, Wu [5] employed finite element simulation and analysis to examine the dynamic distribution of the surrounding rock plastic zone. The aforementioned investigation was performed in the presence of three working conditions of no support, primary support, and secondary lining, confirming that the numerical simulation would be capable of reflecting the plastic zone distribution of the surrounding rock very intuitively. Guo et al. [6] analyzed the distribution pattern of plastic zones in circular tunnels through theoretical analysis and concluded that the general patterns of plastic zones in tunnels in the presence of various surrounding pressure conditions are circular, elliptical, and butterfly. They also deduced criteria for determining various plastic zone morphologies by conceptualizing the plastic zone morphology factor and checking the accuracy of theoretical calculations using FLAC^{3D}. Lai and Zhang [7] took Songjiagou Tunnel No. 1 of the Chengdu–Chongqing Expressway as the engineering background and calculated the arch settlement, convergence of surrounding rock, plastic zone, vertical stress of surrounding rock, and minimum primary support stress for three types of in situ expansion methods for the existing tunnels. It is suggested to close the support structure into a ring as soon as possible after the expansion is completed, which is not only useful for the stability of the surrounding rock but also for the groundwater protection in the surrounding rocks near the tunnel. Yang et al. [8] examined the mechanical properties of the surrounding rock of the unilateral tunnel expansion through analytical calculations. To this end, an analytical procedure was proposed for calculating the mechanical properties of the surrounding rock of the in situ expansion tunnel, seeing that the support of the surrounding rock plays a vital role in stabilizing the surrounding rock of the tunnel. Based on the surrounding soft rock highway tunnel on top of the mountain, Wang et al. [9] constructed various 3D computational models to demonstrate the reasonableness, comprehensiveness, and superiority of the effect of the extended excavation support construction measures on the stress characteristics of the primary support structure. Subsequently, the mechanical behaviors of the extended excavation support and the primary support were investigated in a more systematic way. Li et al. [10] utilized the finite element method of stratum–structure interaction to study the mechanical mechanism of shield tunnel construction with asymmetric excavation of both sides of the central tunnel and asymmetric demolition of both sides of the K-tube plate. The results revealed that the diaphragm wall was subjected to obvious bias pressure under asymmetric excavation of both sides of the central tunnel and asymmetric demolition of both sides of the K-tube sheet. Zeng et al. [11] exploited the Chongqing Huofengshan Tunnel as an engineering background and explored the tunnel deformation and supporting structure force characteristics of three distinct variable sections of the Huofengshan left tunnel by combining numerical simulation, model test, and field monitoring. Additionally, the effects of the tunneling process on the uneven settlement of the surface building were also assessed before and after optimization. In addition to the above literature, some investigations have been devoted to the examination of changes in strength, hydraulic conductivity, and microstructure of the surrounding rock during tunnel expansion. For instance, Bian et al. [12] examined the mechanical properties and water migration patterns of soil stabilized with superabsorbent polymers in wetting–drying cycles and found that these polymers are capable of effectively increasing the compressive and shear strength of soil, reducing the coefficients of hydraulic conductivity and porosity of soils, and improving the microstructure of soils. In another work, Bian et al. [13] investigated the role of plasticity in the strength behavior of cement–phosphogypsum stabilized soils, establishing a strength model considering plasticity. In continuing, the effects of cement dose, phosphogypsum dose, curing time, and moisture content on the strength of soils were inclusively addressed and discussed. Zhang et al. [14] analyzed the effect of clay fraction on the mechanical properties and microstructural characteristics of waste stone bricks and found that increasing the clay fraction leads to an increase in both the compressive and flexural strengths of stone bricks, improving the pore structure and mineral composition of waste stone fine bricks.

The above literature survey reveals the scientific nature of studying the plastic zone of the surrounding rock during tunnel expansion and the importance of investigating the distribution of plastic zone in tunnels, while at this stage, fewer studies have been devoted to the distribution of plastic zone in expanded tunnels. In addition, changes in strength, hydraulic conductivity, and microstructure of the surrounding rock also affect the effectiveness and safety of tunnel expansion, and therefore various surrounding rock materials and remedial measures should be considered. Herein, with the background of the Huang Shan Dong Tunnel Rehabilitation Project of Yiba highway, a computational model for various surrounding rock grades in the presence of various tunnel expansion approaches is developed based on theoretical analysis and numerical simulation. By studying different dimensions of tunnel expansion and various lateral pressure coefficients, the size and shape of plastic zones of existing highway tunnels based on various expansion approaches are deeply scrutinized. The main objective is to provide a rational optimization scheme for the design and construction parameters of tunnel support. The aim of this study is to provide important theoretical and engineering information for rational optimization of anchor support and shotcrete parameters for tunnel extension projects.

2. Mechanical Analysis of Expanded Bored Tunnels

2.1. Initial Mechanical Effects of Existing Tunnels. In the process of tunnel expansion and excavation, localized rock and soil stripping destroys the initial equilibrium of the surrounding rock, which is acted upon by various degrees of disturbances, so that the intensity and direction of its stresses alter. The stress field of the surrounding rock is adjusted to a certain extent under external disturbance (i.e., stress redistribution), and the result is commonly considered through a special field, the so-called secondary stress field. This stress field is closely related to the shape, size, burial depth, construction technology, initial stress field of the surrounding rock, and structural characteristics of the surrounding rock; amongst these factors, the method used for tunnel expansion and excavation has the greatest impact. After the tunnel is excavated, the tunnel should be appropriately resupported. The support structure leads to the reduction of the stress on the surrounding rock and thus forms a cubic stress field.

In conducting theoretical analysis, it is often necessary to make some assumptions and simplifications. In this article, the surrounding rock is considered an ideal elastic–plastic body, and the following assumptions are made:

(1) The surrounding rocks studied in this article comply with the assumptions of continuity, homogeneity, and isotropy.
(2) The effect of the ground on the tunnel is ignored, and the ground is treated as an infinite plane.
(3) The problem of burial depth, which affects the weight of the rock mass in the circle, is negligible.
(4) The tunnel construction project is of infinite length and can be considered as a plane-strain problem.
(5) Only the self-gravitational stress of the rock mass is taken into account in the initial stress field.
(6) The rock mass in the plastic zone obeys the Mohr–Coulomb yield criterion and the rock mass strength in the plastic zone is constant.

Due to the presence of initial stresses in the strata, the underground cavern destroys the original equilibrium state in the strata during excavation, causing the stresses to be redistributed around the excavated hairy cavern as well as in the nearby strata. The initial stress state of the surrounding rock is given in Figure 1.

The initial stress at any point in the horizontal stratum is assumed to be:

$$\begin{cases} \sigma_z = \int \gamma(z)dz \\ \sigma_x = \dfrac{\mu}{1-\mu}\sigma_z \\ \tau_{xz} = 0 \end{cases}, \tag{1}$$

where σ_x, σ_z, and τ_{xz} are the stress components, and $\gamma(z)$ is the strain component.

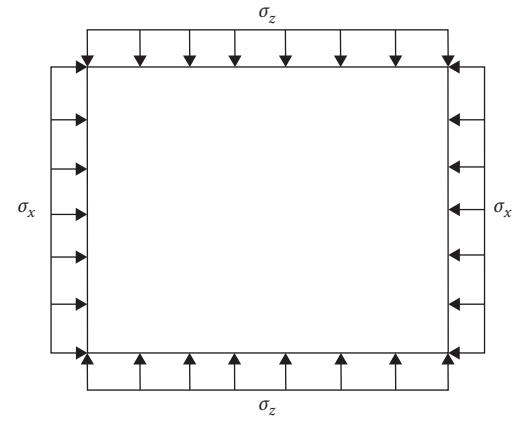

Figure 1: Initial stress state of the surrounding rock.

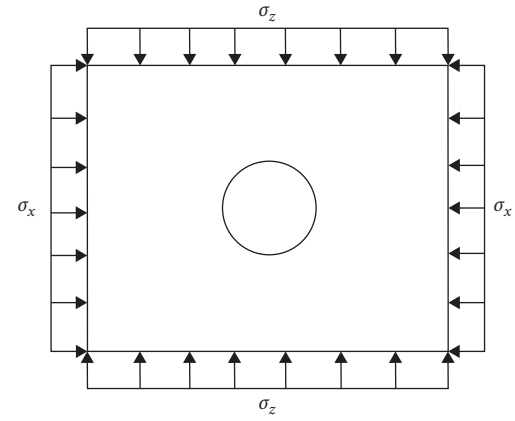

Figure 2: Excavation disturbance dynamics modeling of the surrounding rock.

The initial stress in the surrounding rock in polar coordinates (where r is the polar diameter and θ is the polar angle) can be expressed as follows:

$$\begin{cases} \sigma_r = \dfrac{1}{2}(\sigma_z + \sigma_x) - \dfrac{1}{2}(\sigma_z - \sigma_x)\cos 2\theta \\ \sigma_\theta = \dfrac{1}{2}(\sigma_z + \sigma_x) + \dfrac{1}{2}(\sigma_z - \sigma_x)\cos 2\theta \\ \tau_{r\theta} = \tau_{\theta r} = \dfrac{1}{2}(\sigma_z - \sigma_x)\sin 2\theta \end{cases}, \tag{2}$$

where σ_r and σ_θ are the normal stress.

When the tunnel is expanded, the cavity destroys the original equilibrium state of the strata in the expansion process, which makes the stress redistributed around the expanded cavity as well as in the nearby strata (see Figure 2). In order to simplify the calculation, it is considered that the excavation perturbation of the underground cavern is, mechanically speaking, actually a problem of orifice effect (i.e., a void in a semi-infinite body), so the surrounding stresses are simplified to a homogeneous load acting on the boundary.

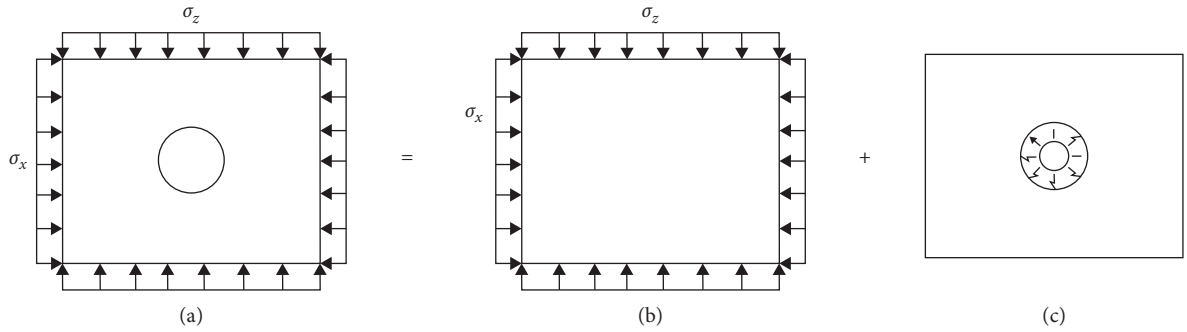

FIGURE 3: Superposition calculation of the secondary stress field of the surrounding rock. (a) Secondary stress field in the perimeter rock after excavation. (b) Initial stress field in the surrounding rock. (c) Disturbed stress field.

In view of the above explanations and assumptions, considering the relationship between the stress function and the stress components, the stress function of the excavation disturbance can be assumed as:

$$\varphi(r,\theta) = f_1(r) + f_2(r)\cos 2\theta, \tag{3}$$

where $f_1(r)$ and $f_2(r)$ are nonlinear functions on r.

By introducing the above equation into the compatibility equations $(\frac{\partial^2}{\partial r^2} + \frac{1}{r}\frac{\partial}{\partial r} + \frac{1}{r^2}\frac{\partial^2}{\partial \theta^2})^2 \varphi(r,\theta) = 0$ yields the following equation:

$$\left[\frac{d^4 f_1(r)}{dr^4} + \frac{2}{r}\frac{d^3 f_1(r)}{dr^3} - \frac{1}{r^2}\frac{d^2 f_1(r)}{dr^2} + \frac{1}{r^3}\frac{df_1(r)}{dr}\right] + \cos 2\theta\left[\frac{d^4 f_2(r)}{dr^4} + \frac{2}{r}\frac{d^3 f_2(r)}{dr^3} - \frac{9}{r^2}\frac{d^2 f_2(r)}{dr^2} + \frac{9}{r^3}\frac{df_2(r)}{dr}\right] = 0. \tag{4}$$

Since Equation (3) should be satisfied for all values of θ, one can arrive at the following equation:

$$\begin{aligned}\left[\frac{d^4 f_1(r)}{dr^4} + \frac{2}{r}\frac{d^3 f_1(r)}{dr^3} - \frac{1}{r^2}\frac{d^2 f_1(r)}{dt^2} + \frac{1}{r^3}\frac{df_1(r)}{dr}\right] &= 0\\ \left[\frac{d^4 f_2(r)}{dr^4} + \frac{2}{r}\frac{d^3 f_2(r)}{dr^3} - \frac{9}{r^2}\frac{d^2 f_2(r)}{dr^2} + \frac{9}{r^3}\frac{d^2 f_2(r)}{dr}\right] &= 0.\end{aligned} \tag{5}$$

By introducing the intermediate variable $r = e^t$, the two equations can be transformed into relations with constant coefficients (where a, b, c, and d are constants). By using the inverse transformation $t = \ln r$, it is possible to reduce Equation (4) to two functions in terms of r with constant coefficients as follows:

$$\begin{aligned} f_1(r) &= a_1 \ln r + b_1 r^2 \ln r + c_1 r^2 + d_1\\ f_2(r) &= a_2 r^4 + b_2 r^2 + c_2 + \frac{d_2}{r^2}.\end{aligned} \tag{6}$$

By introducing Equation (5) to Equation (2), the stress function associated with the excavation phase can be derived as follows:

$$\begin{aligned}\varphi(r,\theta) = a_1 \ln r + b_1 r^2 \ln r + c_1 r^2 + d_1\\ + \left(a_2 r^4 + b_2 r^2 + c_2 + \frac{d_2}{r^2}\right)\cos 2\theta.\end{aligned} \tag{7}$$

It should be noted that an error will be generated in the calculations of the displacement in the case of $\theta = 2k\pi$. Since the error should be removed, it can be concluded that $b_1 = 0$. Therefore, Equation (6) can be reduced as follows:

$$\varphi(r,\theta) = A \ln r + Br^2 + \left(Cr^2 + Dr^4 + \frac{E}{r^2} + F\right)\cos 2\theta. \tag{8}$$

By introducing the above equation into the equation used for solving the stress component in polar coordinates, the stress components pertinent to this stress function take the following form:

$$\begin{cases}\sigma_r = \dfrac{A}{r^2} + 2B + (-2C - 6Er^{-4} - 4Fr^{-2})\cos 2\theta\\ \sigma_\theta = -\dfrac{A}{r^2} + 2B + (2C + 12Dr^2 + 6Er^{-4})\cos 2\theta\\ \tau_{r\theta} = (2C + 6Dr^2 - 6Er^{-4} + 2Fr^{-2})\sin 2\theta\end{cases}, \tag{9}$$

where A, B, C, D, E, and F are constants to be determined by imposing the boundary conditions.

2.2. Secondary Stresses in the Elastic Zone of the Surrounding Rock of the Expanded Excavation of the Existing Tunnel. When tunnel expansion is carried out, its excavation process makes a disturbance in the equilibrium of the initial stress field. The excavation of rock surrounding the tunnel is equivalent to the hole stress concentration problem, implying that the secondary stress field of the surrounding rock is superimposed by the initial stress field and the disturbed stress field caused by the hole excavation. A specific superposition has been presented in Figure 3.

From the superposition, it can be seen that the stress at the hole surface should be zero after the excavation of the cave. Due to the existence of initial ground stress, in order to satisfy the state of zero stress at the hole surface, it is necessary to apply a load around the rock opening that is opposite

to the initial ground stress, so that there would be a specific stress boundary condition for the hole as follows:

$$\begin{cases} \sigma_r|_{r=a} = \Delta\sigma_r = -\dfrac{1}{2}(\sigma_z + \sigma_x) + \dfrac{1}{2}(\sigma_z - \sigma_x)\cos 2\theta|_{r=a} \\ \tau_{r\theta}|_{r=a} = \Delta\tau_{r\theta} = -\dfrac{1}{2}(\sigma_z - \sigma_x)\sin 2\theta|_{r=a}, \end{cases} \tag{10}$$

where a represents the radius of the hole.

In view of St. Venant's principle, the stresses at the radius of infinity are not affected by the abovementioned disturbances; therefore, the radial stress, circumferential stress, and shear stress due to the hole at the radius of infinity take zero values, so we can arrive at $B = C = D = 0$ for the stress components. Additionally, by substituting Equation (9), we can arrive at the disturbed stresses around the hole after the entrance excavation:

$$\begin{cases} \sigma_r(r,\theta) = -\dfrac{1}{2}(\sigma_z + \sigma_x)\left(\dfrac{\alpha}{r}\right)^2 - \dfrac{1}{2}(\sigma_z - \sigma_x)\left(\dfrac{3a^4}{r^4} - \dfrac{4a^2}{r^2}\right)\cos 2\theta \\ \sigma_\theta(r,\theta) = \dfrac{1}{2}(\sigma_z + \sigma_x)\left(\dfrac{\alpha}{r}\right)^2 + \dfrac{1}{2}(\sigma_z - \sigma_x)\dfrac{3a^4}{r^4}\cos 2\theta \\ \tau_{r\theta} = -\dfrac{1}{2}(\sigma_z - \sigma_x)\left(\dfrac{3a^4}{r^4} - \dfrac{2a^2}{r^2}\right)\sin 2\theta. \end{cases} \tag{11}$$

Superimposing the above equation with the initial stress in the surrounding rock gives the secondary stress field in the elastic zone of the hole excavation as follows:

$$\begin{cases} \sigma_r(r,\theta) = \dfrac{1}{2}(\sigma_z + \sigma_x)\left(1 - \dfrac{\alpha}{r}\right)^2 - \dfrac{1}{2}(\sigma_z - \sigma_x)\left(1 + \dfrac{3a^4}{r^4} - \dfrac{4a^2}{r^2}\right) \\ \qquad \cos 2\theta \\ \sigma_\theta(r,\theta) = \dfrac{1}{2}(\sigma_z + \sigma_x)\left(1 + \dfrac{\alpha}{r}\right)^2 + \dfrac{1}{2}(\sigma_z - \sigma_x)\left(1 + \dfrac{3a^4}{r^4}\right)\cos 2\theta \\ \tau_{r\theta} = \dfrac{1}{2}(\sigma_z - \sigma_x)\left(1 - \dfrac{3a^4}{r^4} + \dfrac{2a^2}{r^2}\right)\sin 2\theta. \end{cases} \tag{12}$$

2.3. Secondary Stresses in the Plastic Zone of the Tunnel Surrounding Rock. The yield criterion is the criterion for determining whether the surrounding rock has entered a state of yielding. The yield surface is the critical criterion for the principal stress of the material. If the stress state of a point is within the yield surface, the point is in the elastic deformation stage; if it is on the yield surface, the point enters the plastic deformation stage. This paper utilizes Mohr–Coulomb yielding criterion to determine whether the surrounding rock enters the plastic state:

$$\sigma_1 = \xi\sigma_3 + \sigma_c, \tag{13}$$

where σ_1 is the maximum principal stress, σ_3 is the minimum principal stress, σ_c is the theoretical uniaxial compressive strength, which can be considered as $2c\cos\varphi/(1-\sin\varphi)$, and ξ is the slope of the intensity line, which can be taken $(1+\sin\varphi)/(1-\sin\varphi)$.

When the lateral pressure coefficient of the surrounding rock is 1, it can be considered that the tangential stress σ_θ is the maximum principal stress and the radial stress σ_r is the minimum principal stress; therefore, the condition for the rock body to enter the plastic state can be rewritten as the following equation:

$$\sigma_\theta = \xi\sigma_r + \sigma_c. \tag{14}$$

To indicate the distinction in the stress symbols, let us add p to indicate the stress in the plastic zone; then, the static equilibrium equation inside the plastic zone can be stated as:

$$\sigma_{\theta p} = d(r\sigma_{rp})/dr. \tag{15}$$

By introducing Equation (14) into the static equilibrium equation, the following equation is obtained:

$$\begin{aligned} \sigma_{\theta p} &= \frac{\sigma_{\theta p} - \sigma_c}{\xi} + \frac{rd\sigma_{\theta p}}{\xi dr} \\ \frac{d\sigma_{\theta p}}{dr} &- \frac{\xi - 1}{r}\sigma_{\theta p} = \frac{\sigma_c}{r}. \end{aligned} \tag{16}$$

By imposing the boundary conditions $\sigma_{rp} = 0$ at $r = a$, the secondary stress field in the plastic zone can be found to be:

$$\begin{cases} \sigma_{\theta_p} = \dfrac{\sigma_c}{\xi - 1}\left[\xi\left(\dfrac{r}{a}\right)^{\xi-1} - 1\right] \\ \sigma_{r_p} = \dfrac{\sigma_c}{\xi - 1}\left[\left(\dfrac{r}{a}\right)^{\xi-1} - 1\right] \end{cases}. \tag{17}$$

3. Calculation of Elastic–Plastic Zone of the Tunnel Surrounding Rock in the Presence of Various Expansion Methods

3.1. Project Overview. Huangshan Cave Tunnel is located on Yiba highway from K26 + 524.5 to K26 + 762 Road Pile Section, with a total length of 237.5 m, a straight-line distance between the entrance and the exit of the tunnel of 191.5 m, and a maximum depth of about 100 m, which belongs to a short tunnel. The original tunnel had a clear width of 8.5 m and a clear height of 7.125 m and was designed with end-wall portals for the entrance and exit. However, the clear height of the tunnel does not meet the current specification, the height limit of vehicles at the mouth of the tunnel is 3.8 m, and the traffic volume is far more than the 7,500 vehicles specified for secondary roads. So it is no longer able to cope with the current traffic demand and it is necessary to expand the tunnel.

3.2. Finite Element Modeling. To investigate the plastic zone distribution of the surrounding rock under different tunnel expansion methods, let us consider the Huangshan Cave Tunnel Expansion Project as the case study. According to

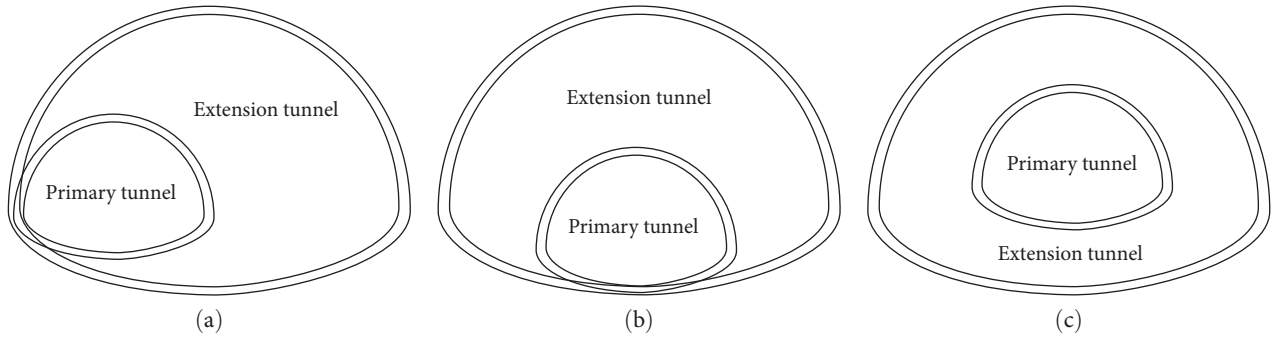

Figure 4: Different expansion approaches of the tunnel: (a) 1SEE, (b) 2SEE, and (c) SEE.

the different levels of the surrounding rock, the tunnel expansion model has been established through the finite element software MIDAS GTS NX. This study is also aimed to develop a finite element model for different approaches used for original tunnel expansion excavation. Different methods of expansion excavation: one-sided expansion excavation (1SEE), two-sided expansion excavation (2SEE), and surrounding expansion excavation (SEE) have been illustrated in Figure 4.

The calculation model for the Huangshan Cave Tunnel before expansion and the mechanical parameters of each material have been presented in Figure 5 and Table 1, respectively.

3.3. Influence of the Expansion Width on the Distribution of Plastic Zone in the Surrounding Rock. The width of the expansion excavation was considered to be 1.5, 3, 4.5, and 6 m. The distribution of plastic zones under unidirectional expansion excavation has been presented in Figure 6.

As the expansion size increases, as shown in Figure 7, the distribution area of the plastic zone also grows, the surface of the plastic zone is gradually smoothed, and the thickness difference of the plastic zone at each point decreases. When the width of the spreading excavation is 1.5 m, the thickness of the plastic zone in each part varies greatly, and when the width of the spreading excavation reaches 4.5 m, the difference gradually decreases. According to the unilateral expansion method, the rock around the tunnel is in a state of bias pressure. In fact, the stress release on the right side of the tunnel and the stress concentration on the left side of the tunnel are detectable, which leads to the plastic zone on the left side of the surrounding rock being larger than that on the right side. As a result, the distribution of the plastic zone on the left and right sides of the tunnel becomes asymmetrical. As the excavation depth increases, the uneven distribution of left and right plastic zones decreases.

The distribution of plastic zones subjected to the 2SEE has been presented in Figure 8.

Similarly, as the expansion excavation size increases, the distribution range of the plastic zone of the surrounding rock increases. According to the 2SEE, the surrounding rock's overall force is relatively balanced, and no bias pressure state is observed, as shown in Figure 9. As a result, the stress is released more uniformly, leading to a symmetrical distribution of the plastic zone in the surrounding rock. The reason

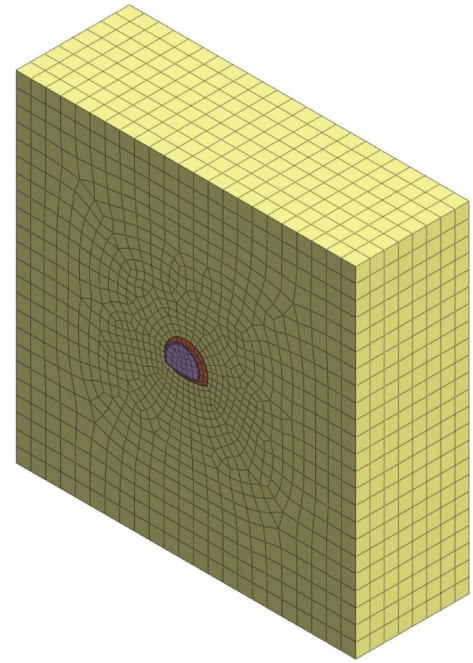

Figure 5: A finite-element model used for mechanical analysis of the Huangshan Cave Tunnel before expansion.

for the significant difference in the thickness of the plastic zone between the arch top and the inverted arch is the 2SEE that mainly targets the upper part of the tunnel. Additionally, the excavation size of the surrounding rock at the arch top is larger than that at the inverted arch, which results in a greater disturbance to the arch top.

The distribution of plasticized zones in the presence of the SEE has been demonstrated in Figure 10.

The plastic zones formed by surrounding expansion and 2SEE are almost similar and symmetrically distributed on both sides of the tunnel axis, while the distribution of the plastic zone of the surrounding rock on the horizontal line of the tunnel is slightly larger than the thickness of the plastic zone of the surrounding rock in the lower part of the tunnel. However, the difference in the thickness of the plastic zone at the arch and the superelevation arch is small because the SEE is a simultaneous excavation of both the arch and the superelevation arch of the tunnel enclosure as shown in Figure 11.

Table 1: Mechanical parameters of the surrounding rock.

Material	Modulus of elasticity (E (GPa))	Poisson ratio (μ)	Density (kN/m³)	Angle of internal friction (degree)	Cohesive force (MPa)
Class III surrounding rock	10.7	0.28	24	44	1.1
Class IV surrounding rock	5.5	0.32	22	30	0.3
Class V surrounding rock	1.1	0.4	18	25	0.1
Mix by spraying	25	0.2	—	—	—
Anchor	210	0.3	—	—	—
Second lining	31	0.2	—	—	—

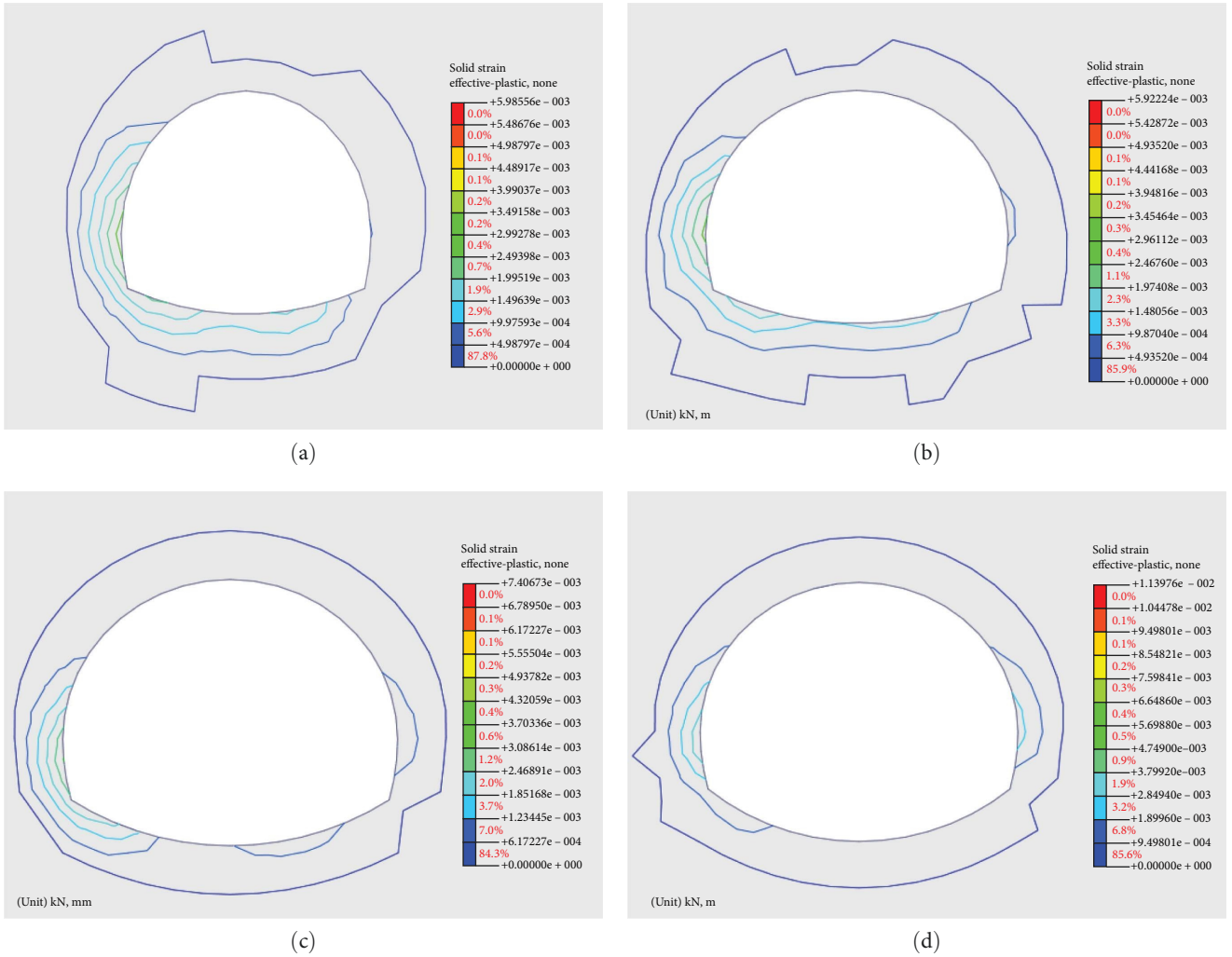

Figure 6: Distribution of the plastic zone in the surrounding rock of 1SEE. (a) Expansion of the excavation by 1.5 m. (b) Expansion of the excavation by 3.0 m. (c) Expansion of the excavation by 4.5 m. (d) Expansion of the excavation by 6.0 m.

This is mainly due to the fact that the SEE is performed by using the same spreading size, so that the stresses at both locations are released at the same time, and thus the range of disturbance to the surrounding rock is comparable.

In summary, when the width of the expansion excavation is not large, the plastic zone of the surrounding rock under the three types of expansion excavation is distributed in a butterfly pattern. This is because of the fact that for tunnel expansion, the arch shoulder and arch foot exhibit more stress release, which makes the distribution range of the plastic zone larger. The range of the plastic zone in the 1SEE is less than that in the 2SEE and the SEE. In fact, 1SEE keeps the side of the main tunnel and spreads the surrounding rock from the other side, which causes less disturbance to the surrounding rock of the tunnel. The plastic zone of both 2SEE and SEE is symmetrically distributed around the tunnel, which is due to the symmetrical and uniform excavation of the surrounding rock on both sides

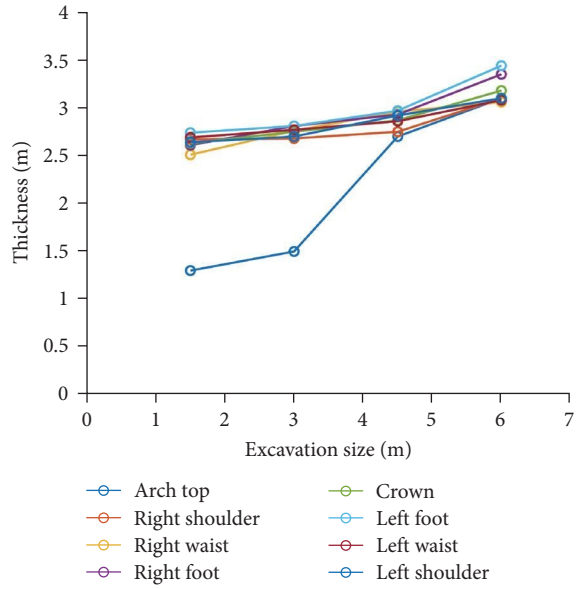

Figure 7: Thickness distribution of the plastic zone in 1SEE.

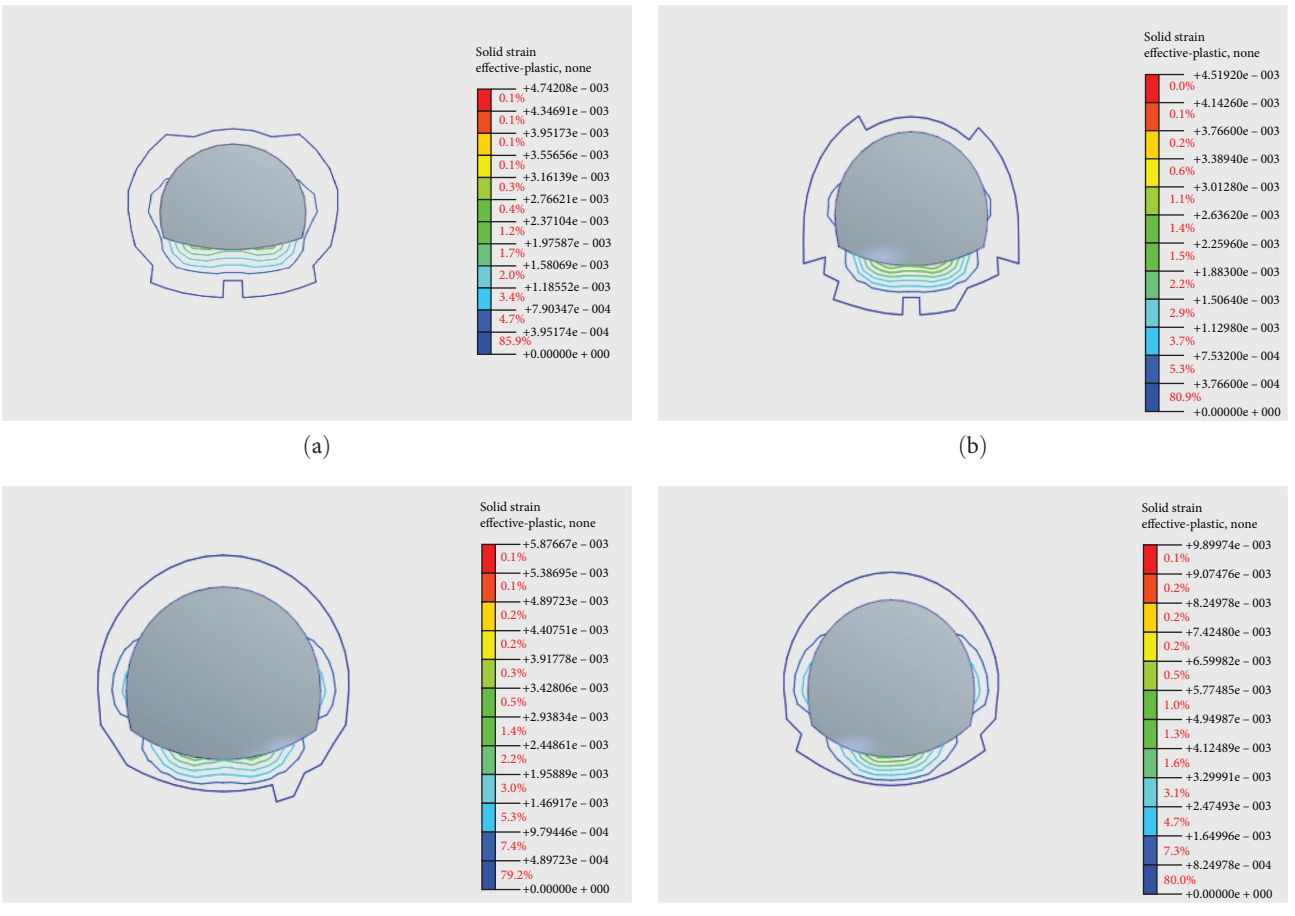

Figure 8: Distribution of the plastic zone of surrounding rock in 2SEE. (a) Expansion of the excavation by 1.5 m. (b) Expansion of the excavation by 3.0 m. (c) Expansion of the excavation by 4.5 m. (d) Expansion of the excavation by 6.0 m.

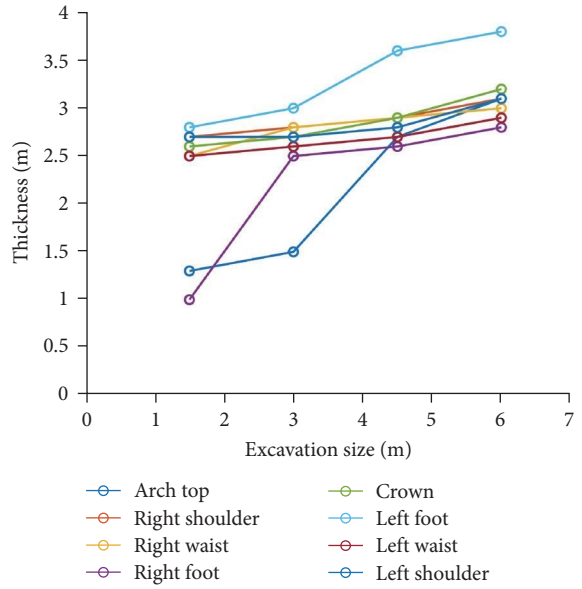

Figure 9: Thickness distribution of the plastic zone in 2SEE.

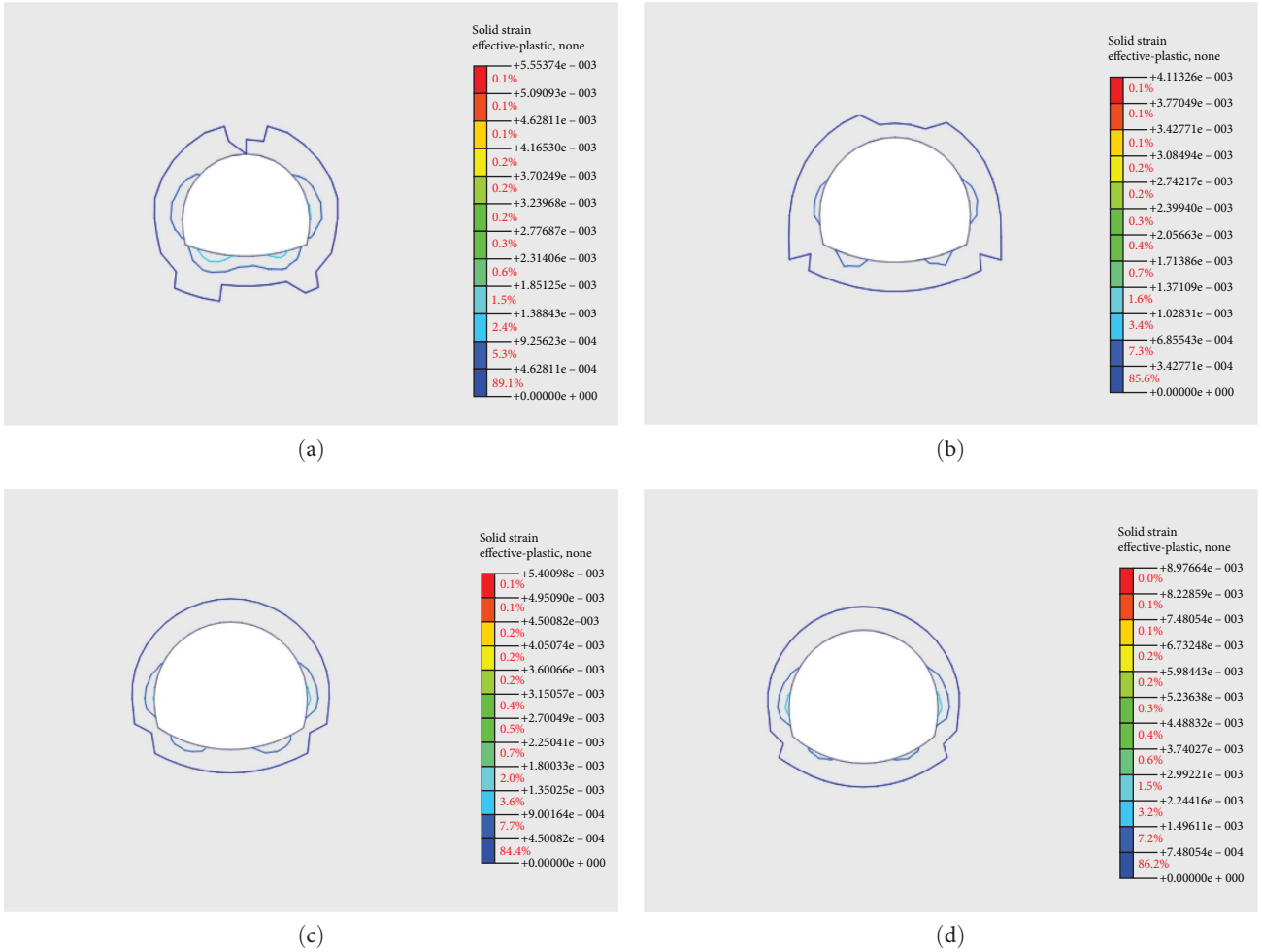

Figure 10: Distribution of the plastic zone of surrounding rock in SEE. (a) Expansion of the excavation by 1.5 m. (b) Expansion of the excavation by 3.0 m. (c) Expansion of the excavation by 4.5 m. (d) Expansion of the excavation by 6.0 m.

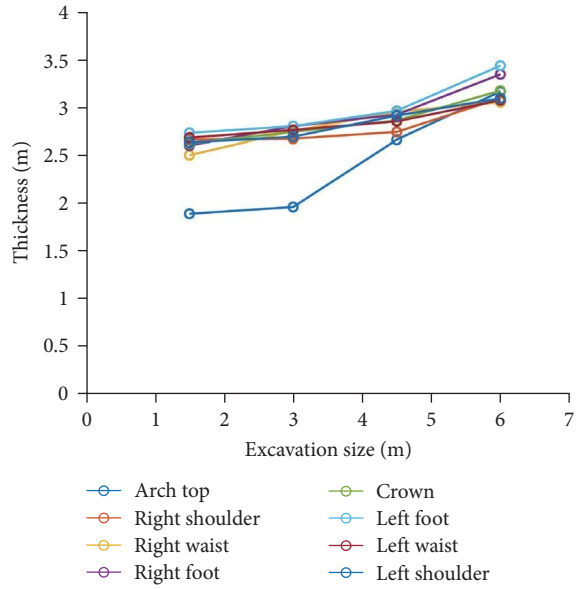

Figure 11: Thickness distribution of the plastic zone in SEE.

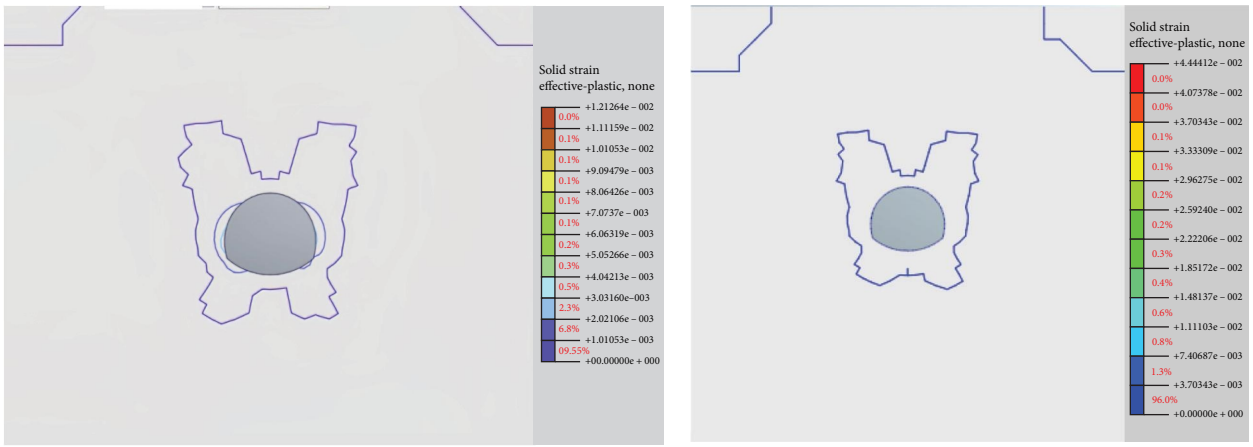

(a) (b)

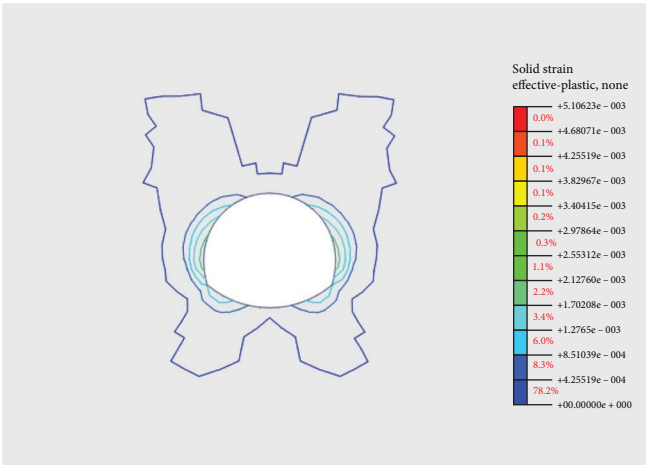

(c)

Figure 12: Distribution of the plastic zone of the surrounding rock in the case of $\lambda = 0.3$: (a) 1SEE, (b) 2SEE, and (c) SEE.

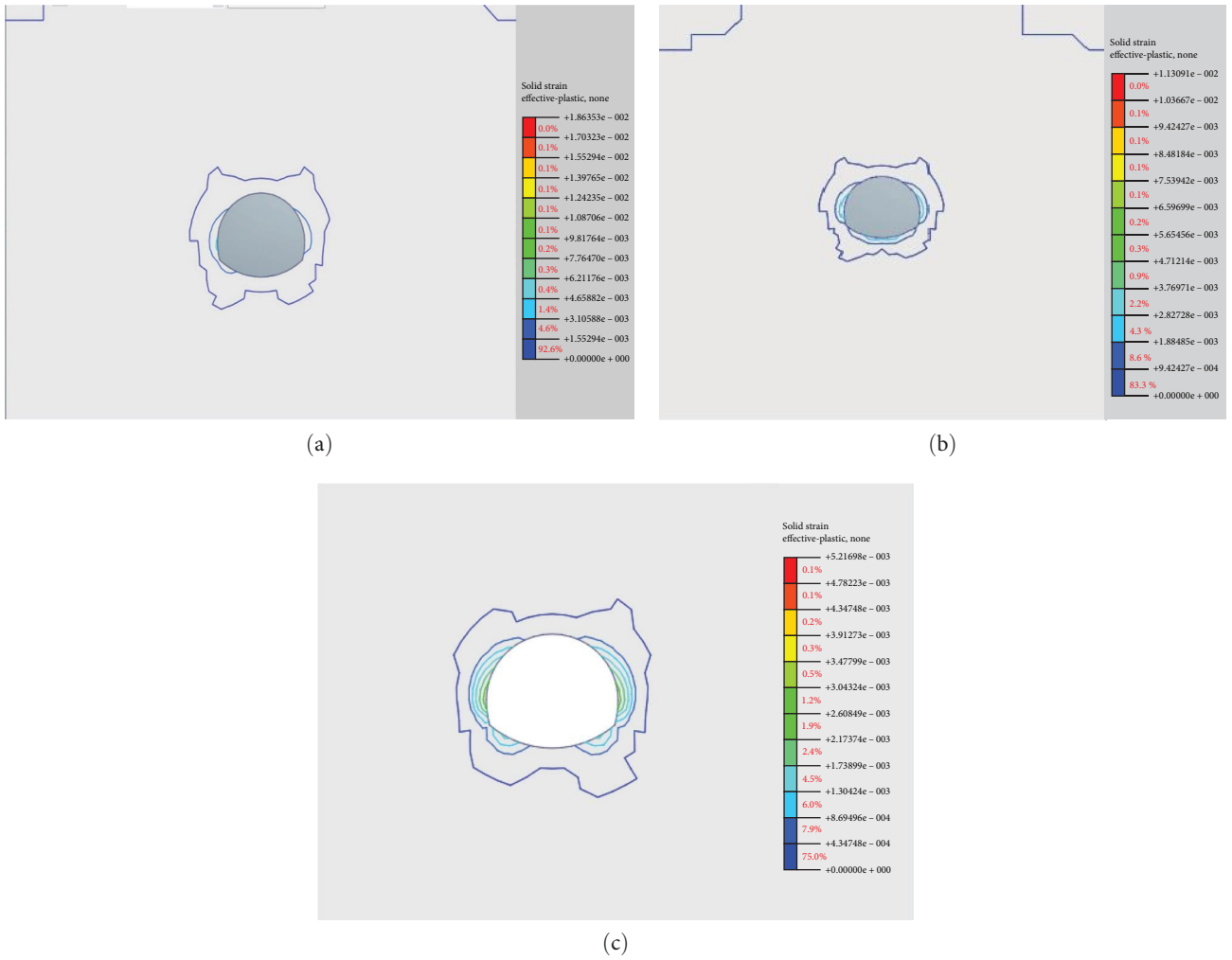

Figure 13: Distribution of the plastic zone of the surrounding rock in the case of $\lambda = 0.5$: (a) 1SEE, (b) 2SEE, and (c) SEE.

of the tunnel in these two approaches and the stress release. In addition, the upward arch of the 2SEE is not damaged, and the stress release is mostly observed at the top of the arch, and the stress of the surrounding rock is relatively concentrated in the upward arch, which makes the settlement of the top of the arch greater than the uplift of the upward arch, and thus the plastic zone has a larger distribution range over the center of the tunnel.

3.4. Influence of Lateral Pressure Coefficient on the Distribution of Plastic Zone in the Surrounding Rock. In order to analyze the effect of the lateral pressure coefficient λ on the distribution of the plastic zone, along with the ground stress environment in which the surrounding rock is located, three modes of the lateral pressure coefficient $\lambda = 0.3$, 0.5, and 1.0 are set [15–17], and the plastic zone distribution is simulated and calculated.

For the case of an expansion size of 6 m for analysis and the lateral pressure coefficient of 0.3, the distribution of the plastic zone of the surrounding rock in three different expansion methods is shown in Figure 12.

In the case of $\lambda = 0.3$, the plastic zone under the three ways of excavation expansion is symmetrically distributed around the tunnel in an "X"-shape about the center of the tunnel, and the plastic zone at the position of the shoulder of the arch and toe is developed along the tunnel with a slope of 45°. Besides, the development zone at the top is obviously larger than that at the bottom, which is mainly because the excavation of the surrounding rock at the top of the tunnel reduces the surrounding rock stresses at the arch shoulder position, making the distribution range of the plastic zone larger. The main reason for this phenomenon is that when the surrounding rock above the tunnel is excavated, the arch shoulder releases more surrounding rock stresses, resulting in the distribution range of the plastic zone being larger. The smaller distribution range of the plastic zone in the high arch is due to the nonuniform ground stress field in both directions. For the case of 1SEE, the thickness of the right arch shoulder and right arch foot is greater than that of the left arch shoulder and left arch, which is mainly due to the fact that the expansion is unilaterally performed to the right. For the case of both 2SEE and SEE, the plastic zone is symmetrically distributed due to symmetrical expansion. As the 2SEE excavates the upper part of the original tunnel, it releases the arch stress, which causes the difference between the plastic zone of the arch and the superelevation arch to be very large.

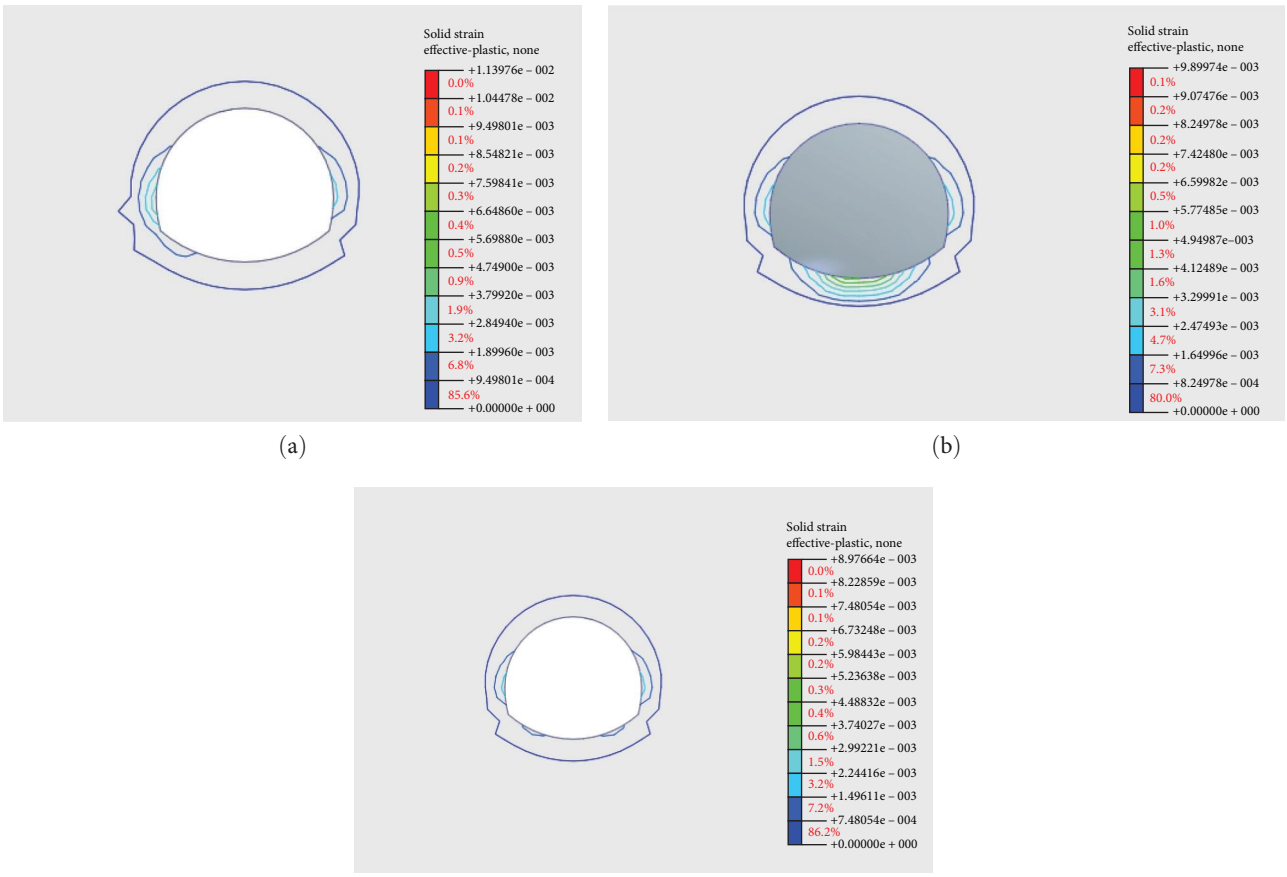

Figure 14: Distribution of the plastic zone of the surrounding rock in the case of $\lambda = 1.0$: (a) 1SEE, (b) 2SEE, and (c) SEE.

However, the SEE incorporates the stress release of the arch and the superelevation arch at the same time, making a small difference in the plastic zone.

In the case of $\lambda = 0.5$, the X-type plastic zone is degraded to a butterfly-type distribution (as shown in Figure 13) mainly because the lateral pressure coefficient increases, the difference between the horizontal and vertical stresses lessens in the tunnel and the distribution range of the plastic zone in the surrounding rock decreases. The difference in the thickness of the plastic zone in the arch and the superelevation arch is reduced under the 2SEE also due to the reduction in the difference between the horizontal and vertical stresses in the tunnel. The difference in the thickness of the plastic zone at the top of the arch and behind the arch is reduced, also due to the reduction of the difference between the horizontal and vertical ground stress. Since SEE has the largest area of excavation for the original tunnel, the formed plastic zone area is also the largest.

In the case of $\lambda = 1.0$, the plastic zone in the presence of three distinct excavation expansion approaches changes from a butterfly type to a regular ellipse, as illustrated in Figure 14. This change is essentially attributed to the fact that with the increase of the lateral pressure coefficient, since the horizontal and vertical stresses in the tunnel are equal, and the distribution range of the surrounding rock plastic zone is further reduced. At this time, due to the increase in the lateral pressure coefficient, the difference in the plastic area between the two-sided expansion arch and the upward arch also decreases. In general, the distribution of the plastic zone of the tunnel around the rock in the cross-section is relatively uniform, and the thickness of the plastic zone does not differ much in each position. The surrounding rock plastic zone is a stable expansion process with a certain symmetry, whereas the distribution of the plastic zone under other lateral pressure coefficients expands in an ellipse form.

3.5. Influence of the Expansion Method on the Thickness of the Plastic Zone of the Surrounding Rock. The thickness of the plastic zone at different locations for the three different methods of expanding the excavation was also evaluated, and the corresponding results have been presented in Figure 15.

With the increase of the expansion width, the thickness of the plastic zone of the surrounding rock increases under different expansion approaches. When expanding the excavation size to 6.0 m, the thickness of the plastic zone is the largest at the arch feet, followed by the shoulder, the arch top, and the inverted arch, and it is smaller at the arch waist. In terms of the increase rate, the thickness arch waist of the plastic zone at the top of the arch and the arch waist increases at a higher rate, and the thickness of the plastic zone at the

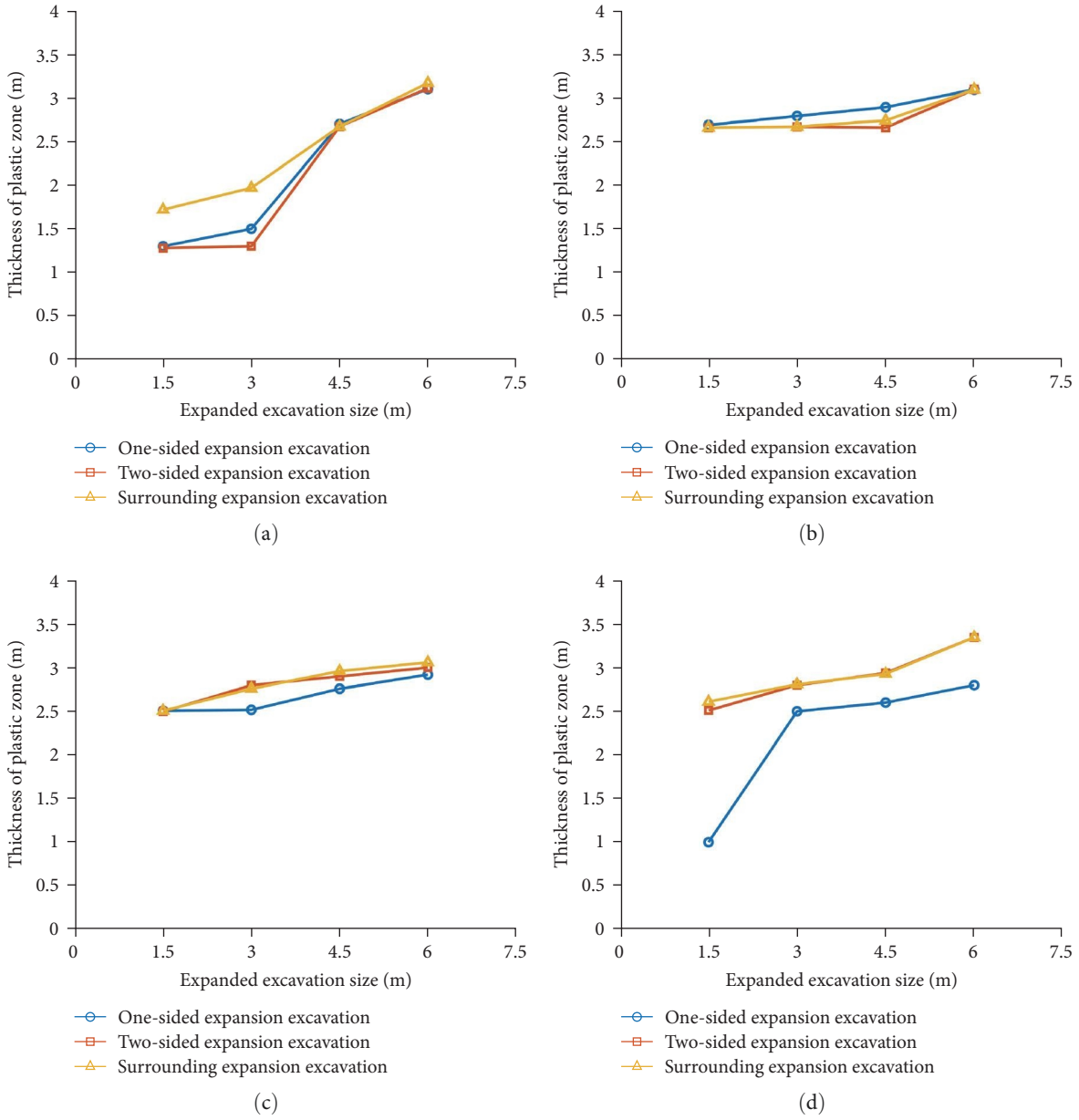

Figure 15: Continued.

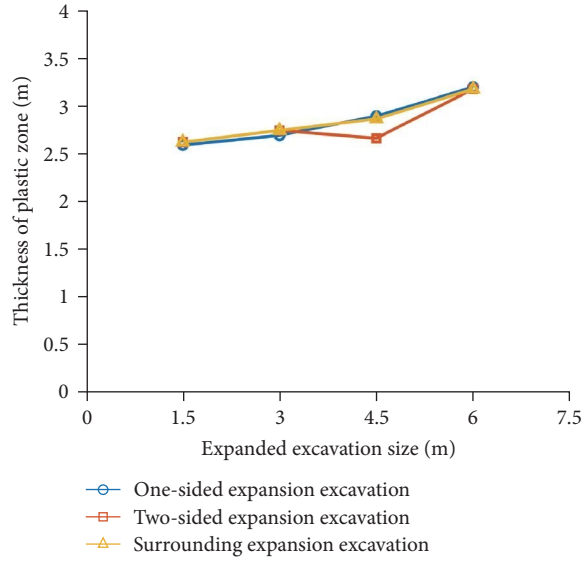

(e)

Figure 15: Thickness of the plastic zones in different positions of the surrounding rock in the presence of various expansion methods: (a) arch top, (b) arch shoulders, (c) arch waist, (d) arch feet, and (e) inverted arch.

arch waist increases more slowly. This is because the arch top and the arch waist are in the higher stress concentration area in the expansion engineering. When the surrounding rock is enlarged, the stress is released rapidly, resulting in the formation and change of plastic zone. The rapid increase of the plastic zone of surrounding rock will lead to the failure of surrounding rock, resulting in the failure of normal construction. Therefore, the support of arch top and the arch waist should be strengthened in time, and the surrounding rock should be supported and maintained. By comparing the three different expansion approaches, the thickness of the plastic zone at the arch feet and the arch waist in 1SEE is smaller than that in the other two approaches because 1SEE is the same for the tunnel on one side of the original tunnel. However, the other side is only for demolishing the original structure or excavating a very small amount of excavation, which is less disturbing to the surrounding rock at the foot of the tunnel arch, and therefore the thickness of the plastic zone is also smaller. The thickness of the plastic zone is more consistent between 2SEE and SEE because both methods do not alter the tunnel centerline in the excavation process, and SEE is based on two-sided expansion on the surrounding rock around the original tunnel. The difference in the thickness of the plastic zone between the two expansion approaches at different locations is also very small.

4. Conclusions

Based on the Huangshan Cave Tunnel Expansion Project, this paper analyzes the stress field composition of the tunnel expansion surrounding rock. To this end, a finite element model is developed via Midas GTS NX software to examine the plastic zone distribution of the surrounding rock of the tunnel under the transformation of existing tunnels using three different expansion excavation approaches. The distribution and thickness of the plastic zone of the expanded tunnel in terms of the expansion width are systematically analyzed, and the main obtained results are as follows:

(1) In general, the plasticity distribution area increases with the increase of the expansion size in all three expansion methods. By comparing the three different expansion methods, 1SEE exhibits the least disturbance to the surrounding rock, and the distribution range of the plasticity zone is also the smallest. However, due to the inconsistency of the left and right forces in the 1SEE, the distribution of the plastic zone is asymmetric, and the right side of the expansion excavation exhibits a wider range of plastic zone, and uneven plastic distribution. The expansion area decreases with the increase of the expansion excavation width. The distribution of the plastic zone of the 2SEE and the SEE is more consistent, and the distribution of the plastic zone in the axial line of the tunnel is symmetrical. Since the vault and the back arch are simultaneously expanded in the presence of the surrounding expansion, the amounts of expansion of the surrounding rock in the vault and the back arch are the same. Further, the extent of disturbance of the surrounding rock is comparable, so that the gap between the range of the plastic zone of the vault and the back arch is smaller than that of the 2SEE. However, the SEE exhibits the largest excavation area for the original tunnel, and the formed plastic zone is also the largest.

(2) The morphology of the plastic zone under three different excavation expansion methods changes from "X"-type to "butterfly"-type and finally to "ellipse"-type by increasing the lateral pressure coefficient, with a more uniform distribution. The main reason

is that with the increase of the lateral pressure coefficient, the horizontal and vertical stresses of the tunnel gradually approach each other, and the distribution of the surrounding rock plastic zone becomes more uniform. The thickness of the right side is larger compared to the left side, which is the result that the 1SEE is carried out on the right side. This issue causes the right side to have more stress than the left side, which makes the thickness of the plastic zone on the left smaller and the thickness of the plastic zone on both sides becomes the same with the growth of the lateral pressure coefficient. Due to the increase in the lateral pressure coefficient, the differences between the plastic zones of the vault and the back arch in the case of 2SEE are reduced.

(3) In the process of increasing the size of the expansion excavation, the thickness of the plastic zone of the surrounding rock based on the three expansion excavation approaches increases, and the thickness of the plastic zone at the arch feet is larger. The thickness of the plastic zone above the arch grows at a higher rate. In 1SEE, the thickness of the plastic zone of the surrounding rock at the arch feet and the arch waist is less than that of 2SEE and SEE. As the expansion excavation width reaches 6 m, in general, the plastic zone of the rock around the tunnel is evenly distributed in the cross-section, and the thickness of the plastic zone is not much different at each position. However, the peak thickness of the plastic zone of the surrounding rock in the presence of SEE is greater than the other two expansion excavation approaches.

According to the above results regarding the expansion and excavation of the tunnel, we should choose more practical methodologies of expansion and excavation for expansion and reconstruction. As a result, the tunnel surrounding rock stress release becomes more reasonable and scientific, and the distribution range of the plastic zone of the surrounding rock is reduced such that the development of the tunnel and the construction of excavations are more secure. In this paper, the influence of groundwater on the formation and distribution of plastic zone in tunnel surrounding rock is not considered.

Data Availability

The authors will supply the relevant data in response to reasonable requests.

Conflicts of Interest

The authors declare that they have no conflicts of interest.

Acknowledgments

This study was funded by the Science and Technology Project of Hubei Provincial Department of Transport in 2020—research on Key Technologies of expanding existing highway tunnels no. 2020-2-1-5.

References

[1] H. Lai, X. Xu, R. Chang, and Y.-L. Xie, "Study on the mechanical characteristics of highway tunnel expansion," *China Journal of Highway and Transport*, vol. 27, no. 1, pp. 84–93, 2014.

[2] Q. Huang, Z. Li, and Y. Wu, "Stress analysis of surrounding rock in shallow tunnel construction," *Journal of Natural Science of Xiangtan University*, vol. 32, no. 1, pp. 25–29, 2010.

[3] C. Zhang, X. Song, W. Wang, Y. Zhang, and S. Yang, "Theoretical analysis and numerical simulation of plastic zone in surrounding rock of bidirectional unequal pressure circular roadway," *Safety in Coal Mines*, vol. 48, no. 11, pp. 217–221, 2017.

[4] Z. Wang, Y. Zhu, and K. Li, "Study on plastic zone of surrounding rock of circular tunnel under non-uniform stress field," *Water Resources and Hydropower Engineering*, vol. 51, no. 11, pp. 197–204, 2020.

[5] J. Wu, "Finite element numerical analysis of plastic zone development in excavation and support of Wuyi tunnel," *Gansu Science and Technology*, vol. 31, no. 10, pp. 77–79, 2015.

[6] X. Guo, N. Ma, X. Zhao, Z. Zhao, and Y. Li, "General form and determination criteria of plastic zone in circular roadway surrounding rock," *Journal of China Coal Society*, vol. 41, no. 8, pp. 1871–1877, 2016.

[7] Y. Lai and S. Zhang, "Research on in-situ expansion and excavation method of tunnels under fluid-solid coupling effect," *Chinese Journal of Underground Space and Engineering*, vol. 15, pp. 311–320, 2019.

[8] B. Yang, C. Lin, Z. Zhang, R. Yin, and Z. Wen, "Analysis of mechanical characteristics of surrounding rock in situ unilateral excavation of tunnels," *Chinese Journal of Underground Space and Engineering*, vol. 14, no. 6, pp. 1458–1465, 2018.

[9] X. Wang, J. Shi, L. Chai, X. Han, and Q. Hu, "Optimization research on construction scheme of weak surrounding rock in Shanziding highway tunnel," *Chinese Journal of Underground Space and Engineering*, vol. 14, pp. 185–192, 2018.

[10] Z. Li, T. Wang, and H. Zheng, "Research on key working conditions control measures for large-diameter shield tunnel excavation in metro stations," *Chinese Journal of Rock Mechanics and Engineering*, vol. 34, no. 9, pp. 1869–1876, 2015.

[11] W. Zeng, X. Peng, L. Zhang, E. Hu, and W. Yang, "Study on stress characteristics of extra-large section variable-section tunnel," *Chinese Journal of Underground Space and Engineering*, vol. 18, no. 6, pp. 2062–2079, 2022.

[12] X. Bian, W. Zhang, X. Li, X. Shi, Y. Deng, and J. Peng, "Changes in strength, hydraulic conductivity and microstructure of superabsorbent polymer stabilized soil subjected to wetting–drying cycles," *Acta Geotechnica*, vol. 17, no. 11, pp. 5043–5057, 2022.

[13] X. Bian, L. Zeng, F. Ji, M. Xie, and Z. Hong, "Plasticity role in strength behavior of cement-phosphogypsum stabilized soils," *Journal of Rock Mechanics and Geotechnical Engineering*, vol. 14, no. 6, pp. 1977–1988, 2022.

[14] S. Zhang, Y. Tan, Y. Deng, H. Ming, H. Li, and J. Wu, "Effect of clay fraction on the mechanical properties and microstructural characteristics of waste rock fine-based brick," *Journal of Cleaner Production*, vol. 424, Article ID 138771, 2023.

[15] X. Chong and W. Qian, "Unified expression model and calculation method for surrounding rock pressure in shallow-buried tunnels," *Journal of Railway Engineering Society*, vol. 39, no. 8, pp. 46–52, 2022.

[16] J. M. Du, Q. Fang, and L. Hai, "Calculation method for surrounding rock pressure in shallow-buried skewed tunnels under surface slope variation," *Journal of Central South University: Science and Technology*, vol. 52, no. 11, pp. 4088–4098, 2021.

[17] F. Hage Chehade and I. Shahrour, "Numerical analysis of the interaction between twin-tunnels: influence of the relative position and construction procedure," *Tunnelling and Underground Space Technology*, vol. 23, no. 2, pp. 210–214, 2008.